INSTITUTE OF PHYSICS PUBLISHING JOURNAL OF PHYSICS: CONDENSED MATTER

J. Phys.: Condens. Matter **14** (2002) 4533–4542 PII: S0953-8984(02)30766-5

The role of Coulomb correlation in magnetic and transport properties of doped manganites: $La_{0.5}Sr_{0.5}MnO_3$ and $LaSr_2Mn_2O_7$

Julia E Medvedeva[1,2], Vladimir I Anisimov[2], Oleg N Mryasov[3] and Arthur J Freeman[1]

[1] Department of Physics and Astronomy, Northwestern University, Evanston, IL 60208-3112, USA
[2] Institute of Metal Physics, Yekaterinburg 620219, Russia
[3] Seagate Research, Pittsburgh, PA 15203, USA

Received 8 November 2001, in final form 31 January 2002
Published 18 April 2002
Online at stacks.iop.org/JPhysCM/14/4533

Abstract

Results of local spin-density approximation (LSDA) and LSDA+U calculations of the electronic structure and magnetic configurations of the 50% hole-doped pseudocubic perovskite $La_{0.5}Sr_{0.5}MnO_3$ and double-layered $LaSr_2Mn_2O_7$ are presented. We demonstrate that the on-site Coulomb correlation (U) of Mn d electrons has a very different influence on the (i) band structures, (ii) magnetic ground states, (iii) interlayer exchange interactions, and (iv) anisotropy of the electrical transport in these two manganites. A p–d hybridization analysis is employed to look for possible explanations for the LSDA failing to predict the observed magnetic and transport properties of the double-layered compound—in contrast to the case for the doped perovskite manganite.

1. Introduction

The half-doped manganites $La_{0.5}Sr_{0.5}MnO_3$ and $LaSr_2Mn_2O_7$ belong to the Ruddlesden–Popper family [1], $(R, A)_{n+1}Mn_nO_{3n+1}$, which has been attracting intense interest due to the itinerant doped carriers that give rise to a variety of interesting physical phenomena, notably colossal magnetoresistance (CMR). One of the most striking properties of the double-layered manganites, $La_{2-2x}Sr_{1+2x}Mn_2O_7$, is the extremely large magnetoresistance, which is much larger than that for prototypical perovskite systems: it was found [2] in 40% doped $La_{2-2x}Sr_{1+2x}Mn_2O_7$ that the resistivity ratio reaches ∼20 000% at 7 T above T_c, whereas [3] for $La_{0.6}Sr_{0.4}MnO_3$ $\rho(0)/\rho(H) \sim 200\%$ at 15 T. The main difference between 3D perovskite and 2D layered compounds arises from the change of dimensionality (n) of the crystal structure connected with the number of MnO_6 layers along the c-direction ($n = \infty$ for pseudocubic perovskite systems and $n = 2$ for double-layered manganites), which in turn has a strong influence on their magnetic and transport properties [2, 4–7]. Measurements and comparisons

of characteristic features (e.g., the strong anisotropy of the electrical (magneto)transport and magnetostriction, and the 2D character of the magnetism caused by the reduction of the exchange coupling between the Mn ions along the *c*-direction in the double-layered manganites) suggested that both the anisotropic transfer interaction and the two-dimensional spin correlation have a strong influence on the CMR properties in layered manganites [2].

The pseudocubic perovskites, $La_{1-x}Sr_xMnO_3$, have an insulating paramagnetic phase at high temperature and a metallic ferromagnetic phase at low temperature over a wide range of hole doping [3, 8]. The strong coupling between the magnetic ordering and the electrical conductivity demonstrates the strong relationship between the electrical resistivity and the spin alignment which has been explained by the double-exchange mechanism arising from the Mn^{3+}/Mn^{4+} mixed valence. In comparison to these pseudocubic perovskites, the double-layered structures ($La_{2-2x}Sr_{1+2x}Mn_2O_7$) with their two-dimensional networks of MnO_6 octahedra have a reduced exchange coupling between the Mn ions along the *c*-direction. Indeed, in the double-layered case consisting of two perovskite blocks separated by an intervening insulating layer of (La, Sr)O ions along the *c*-axis, the balance between antiferromagnetism and ferromagnetism is very sensitive to e_g band filling [9]. Bilayer $La_{2-2x}Sr_{1+2x}Mn_2O_7$ demonstrates ferromagnetism in a doping range $x < 0.39$, a canted antiferromagnetic structure for a hole concentration $0.39 < x < 0.48$, and layered antiferromagnetic states for $x > 0.48$ [10, 11].

An important issue in the theory of CMR oxides is the role of Coulomb correlation, since an accurate treatment of correlation may significantly affect the balance between ferromagnetic and antiferromagnetic interactions and hence the magnetic ground state. According to our previous investigations [12], where we demonstrated that the on-site Coulomb correlation of Mn d electrons significantly modifies the electronic structure, magnetic ordering, and interlayer exchange interactions and promotes strong electronic transport anisotropy in 50% doped $LaSr_2Mn_2O_7$, the experimentally observed magnetic ordering is reproduced within LSDA + U calculations only for $U \geqslant 7$ eV. This is in contrast with the case for the CMR perovskite 3D manganites ($LaMnO_3$, (La, Sr)MnO_3 systems) where LSDA theory correctly predicts the magnetic ground state [13, 14].

Considering two 50% doped manganites—the double-layered $LaSr_2Mn_2O_7$ and the pseudocubic perovskite $La_{0.5}Sr_{0.5}MnO_3$—we outline here the main similarities of and differences between their characteristic properties:

(i) Both manganites formally consist of $Mn^{3.5+}$ ions surrounded by oxygen octahedra, and so in a high-spin configuration the majority t_{2g} states are filled and the electrically active orbitals are $d_{x^2-y^2}$ and $d_{3z^2-r^2}$.

(ii) The dynamical Jahn–Teller (JT) effect is absent for both systems; $\Delta_{JT} = D(\text{Mn–O}_{\text{apical}})/D(\text{Mn–O}_{\text{planar}})$, where D(Mn–O) is the manganese–oxygen distance, is equal to 1.004 and 1.001 for $La_{0.5}Sr_{0.5}MnO_3$ and $LaSr_2Mn_2O_7$, respectively. However, it should be noted here that due to an intervening layer of (La, Sr)O ions along the *c*-axis in the latter manganite, its MnO_6 octahedra are slightly distorted, having different distances between Mn and apical oxygens. Hence, in contrast to the 3D perovskite manganites which have two types of oxygen atom (apical and planar), there are three oxygen types in the double-layered manganites—two apical and one planar.

(iii) The resistivity of $La_{0.5}Sr_{0.5}MnO_3$ is of the order of 10^{-3} Ω cm with a flat temperature dependence [8], whereas for $LaSr_2Mn_2O_7$ the *ab*-plane resistivity is 10^0–10^{-1} Ω cm [15] and the resistivity perpendicular to the layer is $\sim 10^2$ times larger; in addition, according to previous theoretical work [12–14, 16] both are half-metals.

(iv) They have different magnetic orderings: $La_{0.5}Sr_{0.5}MnO_3$ is a ferromagnet (FM), while $LaSr_2Mn_2O_7$ is an A-type antiferromagnet (AFM) (the magnetic moments lie in the

ab-plane and couple ferromagnetically within the single MnO_2 layer, but show AFM order between layers).

(v) As mentioned above, the different influence of the on-site Coulomb correlation on the magnetic ordering in these manganites has been established in previous calculations.

In this paper, on the basis of comprehensive analyses of the crystal structures, electronic structures, and magnetic configurations of the double-layered $LaSr_2Mn_2O_7$ and pseudocubic perovskite $La_{0.5}Sr_{0.5}MnO_3$ compounds, we establish the mechanisms governing the band formation in these manganites and the different roles of the on-site Coulomb correlation in relation to the electronic, magnetic, and transport properties. For both compounds, we consider the total-energy difference between FM and AFM spin configurations for the Coulomb correlation parameter, U, equal to 0 and 7 eV. Then, for the ground states of these manganites, we compare the exchange interaction parameters and the most important band characteristics (such as the population of Mn d states near the Fermi level, Mn d sub-bandwidths, and the p–d hybridization) and give a possible reason for the LSDA scheme ($U = 0$) failing to predict the magnetic ground state as well as the electrical transport properties for the double-layered manganite, in contrast to its success for the case of the pseudocubic perovskite manganite.

2. Methodology

The LSDA and LSDA + U calculations were performed in the framework of the linear-muffin-tin-orbital method in the atomic sphere approximation (LMTO-ASA) [17] with the von Barth–Hedin–Janak form [18] for the exchange–correlation potential. The crystal parameters were taken from [19, 20]. From the constrained LSDA supercell calculations [21, 22], we obtained values of the Coulomb and exchange parameters: $U = 7.1$ eV and $J = 0.79$ eV for $La_{0.5}Sr_{0.5}MnO_3$ and $U = 7.2$ eV and $J = 0.78$ eV for $LaSr_2Mn_2O_7$. These are typical values for the transition-metal oxides [23–25].

3. Results and discussion

3.1. Electronic structure, transport anisotropy, and magnetism

As a first step, we performed band-structure calculations for the FM (all atoms in every layer and between layers are ordered ferromagnetically) and the A-type AFM (ferromagnetic layers stacked antiferromagnetically) phases of both $La_{0.5}Sr_{0.5}MnO_3$ and $LaSr_2Mn_2O_7$ by the standard LSDA method. FM spin alignment is found to be preferable from total-energy calculations for both manganites (table 1). The projected densities of states (DOS) for these FM cases look very similar (figure 1): for the majority-spin channel, Mn 3d states of both compounds form the bands between 2.2 eV below E_F and 2.5 eV above E_F. As seen from the figure, the e_g ($x^2 - y^2$ and $3z^2 - r^2$) bands are partially filled, cross E_F, and are rather broad compared to the t_{2g} (xy and degenerate xz, yz) bands which are about 1.2 eV wide and lie 1 eV below E_F.

The exchange interaction splits the Mn 3d states such that the t_{2g} and e_g minority-spin bands are located 2.6 eV higher in energy than the majority-spin states. We obtained a band gap in the minority-spin d bands of around 2.5 eV for both $La_{0.5}Sr_{0.5}MnO_3$ and $LaSr_2Mn_2O_7$—in keeping with the fact that doped perovskite manganites are found to be half-metallic [14,26,27]. Note that E_F in our spin-polarized band-structure calculations of the double-layered manganite was found to lie at the bottom of the t_{2g} minority-spin conduction band (which is in agreement with the full-potential LMTO calculations for $LaSr_2Mn_2O_7$ [16]), and so the LSDA electronic

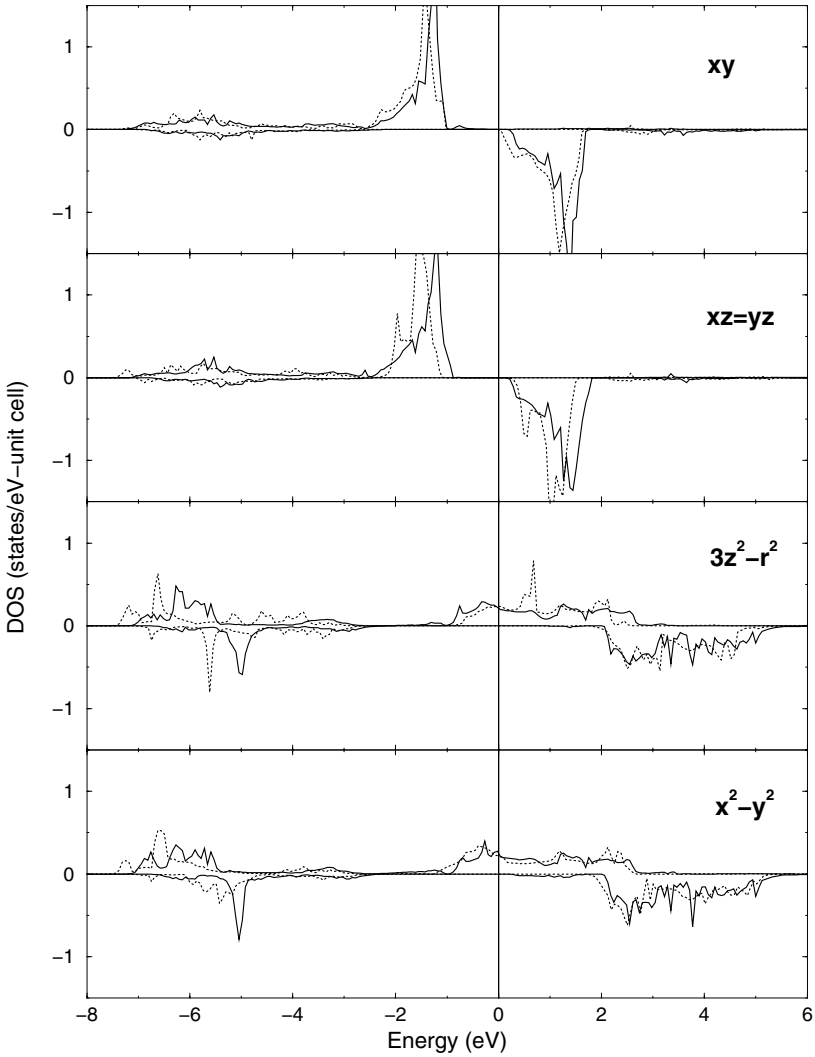

Figure 1. Calculated LSDA Mn d projected densities of states (in states eV^{-1}/unit cell) of FM $La_{0.5}Sr_{0.5}MnO_3$ (solid curve) and $LaSr_2Mn_2O_7$ (dashed curve). The minority-spin contributions are shown as negative states. The Fermi level is located at 0 eV.

band structure just misses being half-metallic (i.e., 100% spin polarization for the conduction electrons).

The crucial role of Coulomb correlation in the stability of the experimentally observed magnetic ground state of $LaSr_2Mn_2O_7$ was established in [12]. We investigated the electronic structure similarities of $LaSr_2Mn_2O_7$ and $La_{0.5}Sr_{0.5}MnO_3$ for both FM and A-type AFM spin alignments in the framework of the LSDA + U method with the calculated U-value of 7 eV. According to the total-energy differences in table 1, the ground state of the perovskite manganite remains ferromagnetic, while the observed A-type AFM ordering in double-layered manganite is found to be energetically more favourable with $U = 7$ eV. (A possible reason for the LSDA failure for the case of the double-layered manganite in contrast to the perovskite will be discussed later.) A comparison of the projected DOSs for the LSDA + U ground states of

Table 1. Total-energy differences, ΔE_{TOT} in meV; the interlayer exchange interaction parameters, J_{dd} in meV; the ratio of the $3z^2 - r^2$ and $x^2 - y^2$ orbital contributions to the DOS at E_F, $N_{x^2-y^2}/N_{3z^2-r^2}$; the ratio of the $3z^2-r^2$ and x^2-y^2 bandwidths, $W_{x^2-y^2}/W_{3z^2-r^2}$; the percentage Mn e_g and O p contributions to the DOS at E_F, N, for $La_{0.5}Sr_{0.5}MnO_3$ and $LaSr_2Mn_2O_7$.

	$La_{0.5}Sr_{0.5}MnO_3$		$LaSr_2Mn_2O_7$	
	$U = 0$	$U = 7$	$U = 0$	$U = 7$
ΔE_{TOT}	+338.9	+473.5	+91.0	−112.4
J_{dd}	+15.28	+94.50	+7.53	−1.84
$N_{x^2-y^2}/N_{3z^2-r^2}$	1.04	0.95	0.94	3.18
$W_{x^2-y^2}/W_{3z^2-r^2}$	1.00	1.00	1.24	2.38
N(Mn $d_{3z^2-r^2}$)	30	24	34	10
N(Mn $d_{x^2-y^2}$)	34	22	32	32
N($O1_{apical}$ ($O2_{apical}$) p_z)	12	18	2 (8)	0 (0)
N($O3_{planar}$ p_x/p_y)	24	36	24	58

$La_{0.5}Sr_{0.5}MnO_3$ (solid curve) and $LaSr_2Mn_2O_7$ (dashed curve) is shown in figure 2. Only majority-spin e_g states contribute to the DOS at E_F. We find the magnetic moment of the primitive unit cell to be equal to 7.00 μ_B. Thus, LSDA + U calculations result in a truly half-metallic state for the double-layered manganite, and so electron conduction is possible only within the majority-spin sublattice.

One of the main differences between the doped pseudocubic perovskite and double-layered manganites, which is clearly seen from figure 2, is the different behaviour of the electrically active states when on-site Coulomb correlation is taken into account. The DOS for the $LaSr_2Mn_2O_7$ e_g states demonstrates (figure 2) a significant difference between $3z^2-r^2$ and $x^2 - y^2$ orbitals in the electron population near E_F, while for $La_{0.5}Sr_{0.5}MnO_3$ the bandwidths and the positions of the band centres of these two e_g orbitals as well as their contributions to the DOS at E_F are very close (figure 2).

In table 1, we presented the ratio between the x^2-y^2 and $3z^2-r^2$ contributions to the DOS at E_F (denoted as $N_{x^2-y^2}/N_{3z^2-r^2}$) calculated in both the LSDA and LSDA + U approaches. The ratio demonstrates the presence of anisotropy in the population of the two e_g states at E_F; and since the situation does not change qualitatively in the 0.3 eV energy window just above E_F (figure 2), we draw the following conclusions about charge transport. For $La_{0.5}Sr_{0.5}MnO_3$, we have 3D conduction; the use of $U = 7$ eV does not result in a large splitting of the e_g states and the number of electrons that contribute to electrical transport remains almost insensitive to the influence of U. This is contrary to the case for $LaSr_2Mn_2O_7$, where for $U = 7$ eV the electron conduction (hopping) along the c-axis (see the small contribution to the DOS at E_F from the $3z^2 - r^2$ orbital in table 1) becomes very small and, thus, on-site correlation treated within the LSDA+U approach promotes 2D type (in-plane) electronic behaviour in the double-layered system—as observed experimentally. Thus, the comparison of the LSDA and LSDA+U band structures for both manganites leads to the following conclusion: the exchange splitting with almost unoccupied minority-spin Mn 3d states and the ligand-field splitting of the t_{2g} and e_g states are the main factors governing band formation in both $La_{0.5}Sr_{0.5}MnO_3$ and $LaSr_2Mn_2O_7$. However, further splitting of the e_g states with increase of U is an essential feature of the layered manganites, but is absent in $La_{0.5}Sr_{0.5}MnO_3$.

The total-energy differences for the two manganites for $U = 0$ and 7 eV shown in table 1 (where the total energy of the FM spin ordering for each U-value is taken to be zero) demonstrate that for the double-layered compound the on-site Mn d electron Coulomb correlations modify the magnetic ordering from FM to A-type AFM—as experimentally observed, while the FM

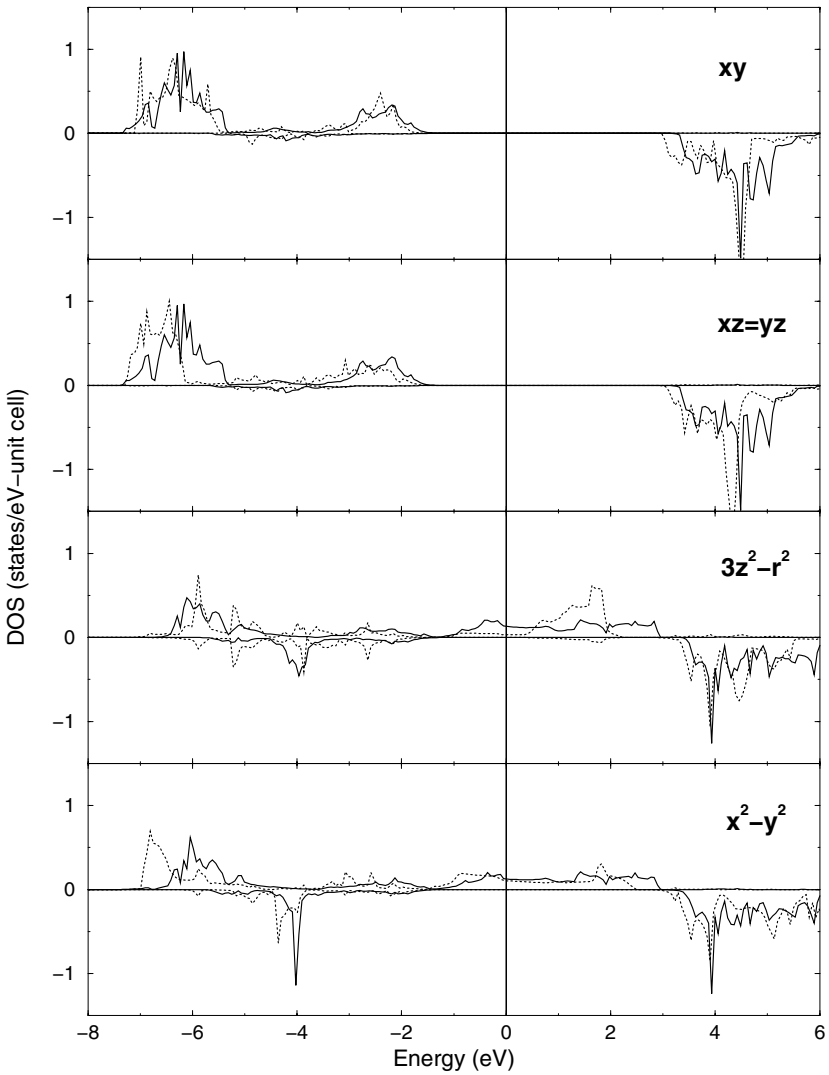

Figure 2. The Mn d projected densities of states (in states eV^{-1}/unit cell) of FM $La_{0.5}Sr_{0.5}MnO_3$ (solid curve) and AFM $LaSr_2Mn_2O_7$ (dashed curve) ground states from LSDA + U calculations with $U = 7$ eV. The minority-spin contributions are shown as negative states. The Fermi level is located at 0 eV.

ground state of the pseudocubic perovskite remains energetically preferred as U is increased. To determine the character of the exchange coupling in these manganites, we calculated the effective exchange interaction parameters (for computational details, see [28]). In table 1, the values of the d–d effective exchange parameters, J_{dd}, between nearest Mn neighbours which belong to the different layers of one bilayer are shown for both U-values. As seen from the table, they follow the magnetic ordering behaviour (obtained from the total-energy differences between FM and AFM configurations) for both compounds. (For more details of the changes of the exchange interaction parameters and the FM–AFM total-energy differences in $LaSr_2Mn_2O_7$ with the increase of U, see [12].)

We interpreted the calculated exchange coupling within the superexchange (SEX) and double-exchange (DEX) models by calculating the e_g sub-bandwidths of the manganite ground states. As can be seen from table 1, where we present the ratio of the $x^2 - y^2$ and $3z^2 - r^2$ bandwidths (denoted as $W_{x^2-y^2}/W_{3z^2-r^2}$), for $La_{0.5}Sr_{0.5}MnO_3$ the e_g bandwidths stay exactly the same with increase of U, and provide positive DEX interactions. We note here that the increase of the ferromagnetic contributions to the exchange interaction energy (cf table 1) may be due to the increase of the e_g bandwidths from 3.4 eV for $U = 0$ to 3.8 eV for $U = 7$ eV and the stronger O p hybridization in the Mn d states—as will be illustrated below. In $LaSr_2Mn_2O_7$, a sharp increase of the $W_{x^2-y^2}/W_{3z^2-r^2}$ ratio coming from the narrowing of the $3z^2-r^2$ bandwidth (table 1 and figure 2) results in the strong splitting of these two e_g sub-bands and so promotes the negative (AFM) contribution to the exchange interaction. Thus, Coulomb correlations have very different influences on pseudocubic and double-layered manganites: for the first, we obtain an increase of the DEX contributions, while for $LaSr_2Mn_2O_7$, U suppresseses the DEX contributions to the interlayer exchange interaction energy and produces the change in magnetic ordering from FM to AFM.

3.2. Significance of p–d hybridization

The degree of O p hybridization with Mn d states plays an important role in the band structure and in the exchange mechanism [13, 29]. We compared the p–d hybridization of $La_{0.5}Sr_{0.5}MnO_3$ and $LaSr_2Mn_2O_7$ for $U = 0$ and 7 eV by calculating the O p contributions to the DOS at the energy windows of corresponding Mn d states. The comparison gives interesting differences between double-layered and perovskite manganites, supporting the results on magnetic and transport properties already discussed above.

According to the qualitative picture of the simple DEX model, an electrically active electron has a finite probability (t) of hopping between ferromagnetically ordered Mn ions, but this hopping vanishes in the case of antiferromagnetic spin alignment due to strong Hund coupling ($t \ll J$). The character of the occupied e_g orbitals, which affects transport and magnetic properties, has been established above, but it is also important to investigate the role of oxygen hybridization in the e_g and t_{2g} orbitals as well [29].

First, we consider the significance of oxygen p hybridization in the electrically active e_g orbitals. For both manganite compounds, two e_g ($3z^2 - r^2$ and $x^2 - y^2$) states and p_x, p_y, p_z oxygen states contribute to the DOS at E_F. In table 1, we present the percentages of these contributions for unit cells consisting of two Mn atoms for both compounds. As expected, only p_z orbitals of apical oxygens (p_x, p_y for planar oxygens) hybridize with 'out-of-plane' $3z^2 - r^2$ ('in-plane' $x^2 - y^2$) d orbitals. Comparing the lowest spin configurations within the LSDA and LSDA + U (as obtained from total-energy differences), we draw the following conclusions: for ferromagnetic $La_{0.5}Sr_{0.5}MnO_3$, we have significant contributions to the DOS at E_F from both apical and planar oxygens, and the on-site Coulomb correlation, resulting in a redistribution of the conduction electrons between e_g and p states, does not change the 3D character of the hopping matrix (table 1). The influence of U on the population picture at E_F in $LaSr_2Mn_2O_7$ is very different. The sharp decrease of the $N_{3z^2-r^2}$ contributions for $U = 7$ eV, that results in suppression of the c-axis transport, occurs together with vanishing apical oxygen contributions at E_F (table 1). This leads to the SEX antiferromagnetic coupling along the c-axis—as was obtained by calculating the interlayer exchange interaction parameters (table 1). In contrast, a sharp increase of the p_x (p_y) hybridization in the $x^2 - y^2$ orbital (due to charge redistribution) provides strong DEX ferromagnetic interactions in the ab-plane.

In addition, the overlap of Mn t_{2g} and O p orbitals in these manganites is an essential factor governing their band formation. In order to compare the p- and d-band overlaps for the

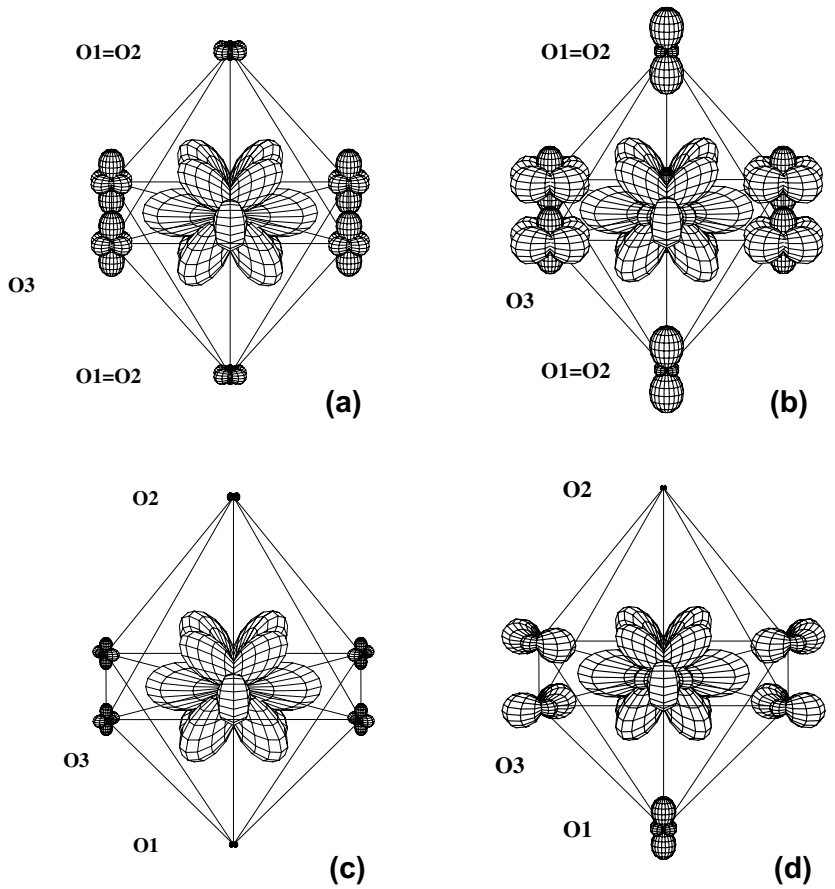

Figure 3. The calculated angular electron-density distribution in the energy window of the corresponding majority-spin t_{2g} states for (*a*) $La_{0.5}Sr_{0.5}MnO_3$, $U = 0$; (*b*) $La_{0.5}Sr_{0.5}MnO_3$, $U = 7$; (*c*) $LaSr_2Mn_2O_7$, $U = 0$ eV, and (*d*) $LaSr_2Mn_2O_7$, $U = 7$ eV. Only one MnO_6 octahedron is shown (for the double-layered manganite it belongs to the upper layer of the bilayer).

perovskite and double-layered compounds, we should, first of all, compare Mn–O distances for these systems. The distances between Mn and apical and planar oxygens in $La_{0.5}Sr_{0.5}MnO_3$ are 1.941 and 1.934 Å, respectively; for the double-layered manganite, they are ∼0.01 Å smaller—1.917 and 1.940 Å for Mn and the apical oxygens, and 1.927 Å for Mn and planar oxygen distances. Such a negligible difference in Mn–O distances serves to stress our results given below.

In figure 3, we present the calculated angular electron-density distribution in the energy window of the corresponding majority-spin t_{2g} states for both manganites. As seen from the figure, the hybridization between Mn d t_{2g} and O p states for $La_{0.5}Sr_{0.5}MnO_3$ exists for both U = 0 and 7 eV, becoming stronger as U is increased (figures 3(*a*) and (*b*)). The same result was obtained for undoped[4] $LaMnO_3$, in which, however, strong JT distortions of MnO_6 octahedra lead to oxygen contributions to t_{2g} Mn states that are more than two times larger than for $La_{0.5}Sr_{0.5}MnO_3$. In contrast to the case for these perovskites, and despite the almost equal Mn–O distances in the doped manganites, LSDA band-structure calculations for

[4] In $LaMnO_3$, the hybridization between Mn t_{2g} and apical oxygen p states stays the same for U = 0 and 8 eV, while contributions to the DOS from planar oxygen increase by 40% when U changes from 0 to 8 eV.

$LaSr_2Mn_2O_7$ gave almost negligible (figure 3(*c*)) O p contributions to the DOS at the energy windows corresponding to t_{2g} states. The p–d hybridization for the double-layered manganite is correctly described only when treated in the LSDA + U approach (figure 3(*d*)): it becomes very strong between Mn and planar oxygens and one of the apical atoms, O1 (which lies between Mn layers of one MnO_6 bilayer unit), while it is suppressed for apical O2 atoms which belong to the (La, Sr) insulating layer as well. Thus, we believe that the absence of p–d hybridization, as an important ingredient in the band formation picture, results in the failure of the LSDA scheme in predicting observed magnetic and transport properties of the double-layered manganite.

The lowered dimensionality of the magnetic interactions in the double-layered system, which was established under the influence of the on-site Coulomb correlation, is also seen from a comparison of two LSDA + U cases for $La_{0.5}Sr_{0.5}MnO_3$ and $LaSr_2Mn_2O_7$ (figures 3(*b*) and (*d*)): in the 3D compound, we have equal contributions to the DOS from all p states (p_x, p_y, and p_z) of planar oxygens, while for the double-layered manganite only p_x (p_y) states of the planar oxygens give significant contributions to the DOS at the energy range corresponding to Mn d t_{2g} states. In addition, the absence of hybridization between Mn d states and apical O2 p states (this oxygen lies at the boundary of the perovskite-type bilayer) makes the whole hybridization picture obtained for double-layered $LaSr_2Mn_2O_7$ for $U = 7$ eV (figure 3(*d*)) in a very good agreement with the structural peculiarity of this compound—namely the existence of two perovskite-type layers separated by a rock-salt-type layer, $(La, Sr)_2O_2$.

4. Summary

In summary, the calculated electronic band structure, exchange interaction parameters, transport properties, and p–d hybridization of double-layered $LaSr_2Mn_2O_7$ are significantly modified by on-site Coulomb correlation, U, resulting in the observed magnetic ground state and transport anisotropy. The comparison with the band characteristics of the 3D perovskite $La_{0.5}Sr_{0.5}MnO_3$ sets these similar doped manganites apart as regards the different roles of the Coulomb correlation in their magnetism and transport properties.

Acknowledgments

The work at Northwestern University was supported by the US Department of Energy (grant No DE-F602-88ER45372) and that at the Institute of Metal Physics was supported by the RFFI (grant No 01-02-17063).

References

[1] Ruddlesden S N and Popper P 1957 *Acta Crystallogr.* **10** 538
[2] Moritomo Y, Asamitsu A, Kuwahara H and Tokura Y 1996 *Nature* **380** 141
[3] Urushibara A, Moritomo Y, Arima T, Asamitsu A, Kido G and Tokura Y 1995 *Phys. Rev.* B **51** 14 103
[4] Kimura T, Tomioka Y, Kuwahara H, Asamitsu A, Tamura M and Tokura Y 1996 *Science* **274** 1698
[5] Perring T G, Aeppli G, Moritomo Y and Tokura Y 1997 *Phys. Rev. Lett.* **78** 3197
[6] Kimura T, Tomioka Y, Asamitsu A and Tokura Y 1998 *Phys. Rev. Lett.* **81** 5920
[7] Rosenkranz S, Osborn R, Mitchell J K, Vasiliu-Doloc L, Lynn J W, Sinha S K and Argyriou D N 1998 *J. Appl. Phys.* **83** 7348
[8] Sundaresan A, Paulose P L, Mallik R and Sampathkumaran E V 1998 *Phys. Rev.* B **57** 2690
[9] Battle P D, Cox D E, Green M A, Millburn J E, Spring L E, Radaelli P G, Rosseinsky M J and Vente J F 1997 *Chem. Mater.* **9** 1042
[10] Kubota M, Fujioka H, Ohoyama K, Hirota K, Moritomo Y, Yoshizawa H and Endoh Y *J. Phys. Chem. Solids* **60** 1161

[11] Moritomo Y, Maruyama Y, Akimoto T and Nakamura A 1998 *J. Phys. Soc. Japan* **67** 405
[12] Medvedeva J E, Anisimov V I, Korotin M K, Mryasov O N and Freeman A J 2001 *J. Magn. Magn. Mater.* **237** 47
[13] Pickett W E and Singh D J 1996 *Phys. Rev.* B **53** 1146
[14] Fang Z, Solovyev I V and Terakura K 2000 *Phys. Rev. Lett.* **84** 3169
[15] Kubota M, Yoshizawa H, Moritomo Y, Fujioka H, Hirota K and Endoh Y 1999 *J. Phys. Soc. Japan* **68** 2202
[16] Huang X, Mryasov O, Novikov D and Freeman A J 2000 *Phys. Rev.* B **62** 13 318
[17] Andersen O K 1975 *Phys. Rev.* B **12** 3060
[18] Barth U, Hedin L and Janak B 1975 *Phys. Rev.* B **12** 1257
[19] Woodward P M, Vogt T, Cox D E, Arulraj A, Rao C N R, Karen P and Cheetham A K 1998 *Chem. Mater.* **10** 3652
[20] Argyriou D N, Bordallo H N, Campbell B J, Cheetham A K, Cox D E, Gardner J S, Hanif K, dos Santos A and Strouse G F 2000 *Phys. Rev.* B **61** 15 269
[21] Gunnarsson O, Andersen O K, Jepsen O and Zaanen J 1989 *Phys. Rev.* B **39** 1708
[22] Anisimov V I and Gunnarsson O 1991 *Phys. Rev.* B **43** 7570
[23] Anisimov V I, Zaanen J and Andersen O K 1991 *Phys. Rev.* B **44** 943
Anisimov V I, Aryasetiawan F and Lichtenstein A I 1997 *J. Phys.: Condens. Matter* **9** 767
[24] Satpathy S, Popovic Z S and Vukajlovic F R 1996 *Phys. Rev. Lett.* **76** 960
[25] Solovyev I, Hamada N and Terakura K 1996 *Phys. Rev.* B **53** 7158
[26] Wei J Y T, Yeh N-C and Vasquez R P 1997 *Phys. Rev. Lett.* **79** 5150
[27] Park J-H, Vescovo E, Kim H-J, Kwon C, Ramesh R and Venkatesan T 1998 *Nature* **392** 794
[28] Lichtenstein A I, Zaanen J and Anisimov V I 1995 *Phys. Rev.* B **52** R5467
[29] Koizumi A, Miyaki S, Kakutani Y, Koizumi H, Hiraoka N, Makoshi K, Sakai N, Hirota K and Murakami Y 2001 *Phys. Rev. Lett.* **86** 5589